Non-targeted identification of tianeptine photodegradation products in water samples by UHPLC-QTOF MS/MS

Enmanuel Cruz Muñoz [a], Veronica Termopoli [a,b], Marco Orlandi [a,b,c], Fabio Gosetti [a,b,c,*]

[a] Department of Earth and Environmental Sciences – DISAT, University of Milano-Bicocca, Piazza della Scienza 1, 20126, Milan, Italy
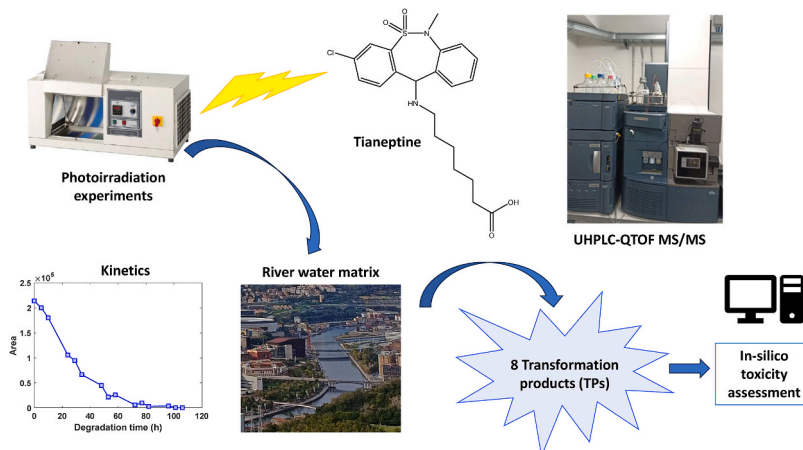[b] NBFC, National Biodiversity Future Center, 90133 Palermo, Italy
[c] POLARIS Research Center, University of Milano-Bicocca, Piazza della Scienza 1, 20126, Milan, Italy

HIGHLIGHTS

- Tianeptine fully photodegrades in water after 106 h of simulated solar irradiation.
- Tianeptine degradation kinetics in ultrapure water and river water are very similar.
- Eight new transformation products of tianeptine were identified by HR MS/MS.
- Same TPs were formed in both ultrapure water and river waters solutions.

GRAPHICAL ABSTRACT

ARTICLE INFO

ABSTRACT

This study aims the characterization of several tianeptine transformation products in ultrapure water by simulated sunlight irradiation. Tianeptine was completely degraded after 106 h of exposition following pseudo-first-order kinetics (half-life time = 12.0 ± 2.4 h). Furthermore, an ultra-high-performance liquid chromatography coupled with a high-resolution quadrupole time-of-flight-mass spectrometry method was developed and fully validated taking into account different method performance parameters for the quantification of tianeptine in river water up to a concentration of 400 pg L^{-1}. Following a non-targeted approach based on mass data-independent acquisition, eight different transformation products not previously reported in the literature were identified and accordingly elucidated, proposing a photodegradation mechanism based on the accurate tandem mass spectrometry information acquired. Irradiation experiments were replicated for a tianeptine solution prepared in a blank river water sample, resulting in the formation of the same transformation products and similar degradation kinetics. In addition, a toxicity assessment of the photoproducts was performed by *in silico* method, being generally all TPs of comparable toxicity to the precursor except for TP1, and showing a similar persistence

in the environment except for TP2 and TP6, while TP4 was the only TP predicted as mutagenic. The developed method was applied for the analysis of four river water samples.

1. Introduction

The consumption of antidepressants for the treatment of depression or anxiety disorders has steadily increased since the COVID-19 pandemic (Diaz-Camal et al., 2022). An alarming prediction by the World Health Organization (WHO) is that depression could be considered the mental illness with the highest overall disability in the world by 2030 (Sindu, 2020). This situation is aggravated by the fact that antidepressants and painkillers are abused in combination with other substances, resulting in cocktails of drugs that cause inhibitory psychotropic effects on the consumer (Diaz-Camal et al., 2022). In fact, the consumption of narcotics has risen over the years, particularly in Countries with the highest citizen income, raising numerous social and environmental problems (Trawiński and Skibiński, 2017; UNODC, 2023).

One of the problems of the use of antidepressant drugs is the environmental impact, since traces of these compounds have been found in surface water of rivers, lakes and seas (Trawiński and Skibiński, 2017). Therefore, it is evident that water contamination has become key in the research and development of methods for the elimination of these substances and reducing the subsequent ecotoxicological damage.

There are many sensitive methodologies for the determination at low concentrations for most of these kinds of drugs (Chen et al., 2023; Zaki et al., 2023; Valdez et al., 2023; Xu et al., 2023). The concentration in surface water mainly depends on the frequency of use, being the concentration range very variable, from few ng L^{-1} to µg L^{-1} (Diaz-Camal et al., 2022). In general, these methods of analysis do not consider the possible transformation products (TPs) that could be generated in the environment by microbial degradation, sunlight irradiation or hydrolysis reactions (Bavumiragira et al., 2022). Some of these TPs can be as toxic or even more toxic than the starting substances, so the monitoring of TPs in the environment becomes essential (Gosetti et al., 2010, 2015, 2018; Bottaro et al., 2008). Only some studies specifically aware of this problem have taken into consideration the persistence of TPs in the environment (Gosetti et al., 2020; Calza et al., 2021; Gornik et al., 2021a; Gros et al., 2015; Metcalfe et al., 2010).

Frequently, studies are focused on the assessment of drug metabolites that are previously known from the initial pharmacokinetic studies carried out before releasing a drug on the market. These metabolites can reach water bodies after hospital, industrial and domestic discharges (Hu et al., 2022). Moreover, antidepressants and their TPs are usually removed in percentages ranging from 18 to 33% (Osawa et al., 2019) or are even not adequately treated and removed in wastewater treatment plants (WWTPs) (Gornik et al., 2021b; Rejek and Grzechulska-Damszel, 2018; Verlicchi et al., 2012). These TPs could be considered emerging pollutants since the persistence of these substances in the environment can lead to the increase of toxic effects on human health or aquatic life (Pivetta et al., 2020; Duan et al., 2022; Ma et al., 2022; Yang et al., 2018; Fong and Molnar, 2013). In addition, sometimes the treatment process itself can cause the metabolites to be transformed back into their precursors leading to higher concentrations in the effluent compared to that of the influent (Calisto and Esteves, 2009; Subedi and Kannan, 2015). Hence, the knowledge of the degradation mechanism of substances of abuse is fundamental to better understanding the fate of these drugs in the environment.

One example of a molecule with an antidepressant effect is tianeptine (TNP), which is the active substance of a tricyclic drug commercialized since 1988 under the name of Zinosal®, Stablon® or Coaxil®, depending on the Country, and used for the treatment of depression and anxiety disorder. The molecular formula of TNP is C$_{21}$H$_{25}$ClN$_2$O$_4$S. This molecule is a secondary amine characterized by aromatic rings and an aliphatic chain with a terminal carboxyl group. Usually presented in the sodic salt form, it is soluble in water and some organic solvents such as ethanol. This antidepressant is orally consumed, and its abuse can cause euphoria, being the psychoactive effect stronger than other associated substances (El Zahran et al., 2018; W. A.JO. DS. C.M, 2001). In 2012, the National Agency for the Safety of Medicines and Health Products (ANSM) in France ruled that there was indeed a risk of abuse and dependence associated with the use of TNP-based antidepressants. Consequently, very often the immediate solution to face this problem seems to be legislative, seeking to limit or avoid the consumption of some drugs even for medical purposes. An example is the situation in Italy, where in 2020 the Italian Ministry of Health included all TNP-based drugs in Table 1 of narcotic substances (Italian Ministry of Health, 2020). Other examples of countries where the commercialization of TNP-derived drugs is no longer permitted are the United States, United Kingdom, Canada, and Australia. Nevertheless, in many Asian Countries or Countries from Europe such as Portugal, France or Spain, its medical use under prescription is still legal (García-García, 2016).

In a gas chromatography-mass spectrometry (GC-MS) study of human urine samples, the pharmacokinetics of TNP in the human body was evaluated and several metabolites were found, being MC5 the main metabolite of TNP and also presenting antidepressant activity (Horlachuk et al., 2019). However, to the best of our knowledge, no studies on the assessment of TNP TPs in waters after natural sunlight irradiation were found in the literature and very few studies assessed the occurrence of the environment, especially in natural waters. One of these few examples reported that TNP was found in seven species of biota fish with a maximum concentration of 0.53 ng g^{-1} of dry weight on the Polish coastline (Świacka et al., 2022). Giebułtowicz et al. (Giebułtowicz and Nałecz-Jawecki, 2014) investigated the presence of TNP in surface water, also providing the predicted environmental concentration of TNP in surface waters based on the 2012 sales of active compound in Poland, which was estimated as 8 ng L^{-1}. In other studies, nineteen surface water samples from the Seine River (Brieudes et al., 2017) and twenty-eight influent wastewater samples collected from each of the four WWTPs in Belgium (Boogaerts et al., 2019) were analyzed, but TNP was not detected in any of the samples. Moreover, in some studies, it was noted that TNP is relatively insensitive to high temperatures, but it can be affected by UV radiation (Khedr, 2007).

This study aims to characterize TNP TPs in water by an ultra-high-performance liquid chromatography quadrupole time-of-flight tandem mass spectrometry (UHPLC- QTOF MS/MS) method. A photodegradation of TNP in water by sunlight-simulated irradiation was carried out imitating environmental conditions that are typical to the north of Spain, where its commercialization is still legal. After developing and validating the proposed method of analysis, four river water samples from the Nervión River (Bilbao, Spain) have been analyzed to check the presence of TNP or its TPs.

2. Materials and methods

2.1. Reagents

TNP sodium salt (≥98 %) was purchased from LGC Standards (Teddington, USA), whereas methanol (UHPLC-MS grade), acetonitrile (UHPLC-MS grade), water (UHPLC-MS grade), and formic acid (LC-MS grade) were acquired from Carlo Erba (Milan, Italy).

2.2. Instrumentation

A Solarbox 3000e (Co.Fo.Me.Gra, Milan, Italy) equipped with a xenon lamp (2500 W), a water-cooled sample tray and a soda-lime glass

UV filter was used to simulate the exposure of the samples to sunlight irradiation. A Universal 320 Centrifuge (Hettich Italia, Milan, Italy) was used for centrifuge operations.
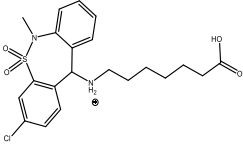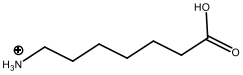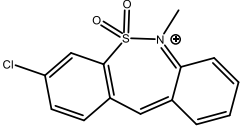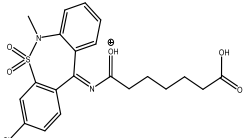
The UHPLC analyses were carried out by ACQUITY UPLC H-Class system (Waters Corporation, Milford, USA) coupled with the Xevo G2-XS QTof Mass Spectrometer (Waters Corp., Milford, MA, USA) through an electrospray ionization (ESI) source. Instrument control and data acquisition were performed by MassLynx 4.2 software (Waters Corporation, Milford, USA) whereas data processing operations such as peak picking, deconvolution, noise level setting, identification of TPs considering accurate mass, as well as isotopic and fragmentation pattern of each detected feature through comparison with the spectral database were carried out by MS-Dial (ver. 5.1.230517) and MS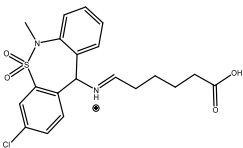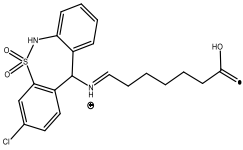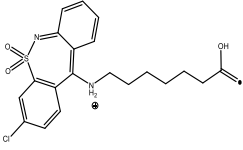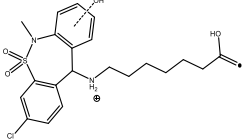-Finder (ver. 3.52), two open-source tools for compound identification in untargeted metabolomics (ht tp://prime.psc.riken.jp/).

2.3. Standard solutions and sample collecting

A TNP standard stock solution (100.0 mgL^{-1}) was prepared in ultrapure water and after proper dilution, it was used for the development

Table 1
Summary of all the identified TPs.

Compound	Molecular formula	Accurate m/z	RT (min)	MS accuracy (ppm)	Chemical structures	Isotopic tolerance (%)	MS/MS accuracy (ppm)	Number of product ions identified
TNP	$C_{21}H_{25}ClN_2O_4S$	437.1306	4.650	1.8		<0.9	<11.8	9
TP1	$C_7H_{15}NO_2$	146.1185	1.523	1.1		<0.9	<11.0	9
TP2	$C_{14}H_{11}ClNO_2S$	292.0203	4.202	0.6		<1.5	<19.5	5
TP3	$C_{21}H_{21}ClN_2O_5S$	449.0948	4.305	3.4		<2.4	<12.7	6
TP4	$C_{21}H_{23}ClN_2O_4S$	435.1128	4.608	2.7		<2.0	<12.0	8
TP5	$C_{20}H_{21}ClN_2O_4S$	421.0975	4.903	2.0		<1.3	<5.2	3
TP6	$C_{20}H_{21}ClN_2O_4S$	421.0988	5.094	2.6		<2.4	<8.4	4
TP7	$C_{20}H_{21}ClN_2O_4S$	421.0986	6.150	0.6		<3.1	<1.2	5
TP8	$C_{21}H_{25}ClN_2O_5S$	453.1233	6.494	2.8		<5.9	<12.1	6

and validation of the UHPLC-MS/MS method. The stock solution was kept at −20 °C in an amber glass vial. For the irradiation experiments, an aqueous solution of TNP (10.0 mg L^{-1}) was freshly prepared.

River water samples were collected from Nervión River (Bilbao, Spain), according to ISO 5667–6:2014 (ISO, 2014) The samples (1.5 L each) were collected at four different points of the river (Fig. S1): river mouth close to the sea (43.321488 N, 3.016796W), industrial area (43.304207 N, 2.980176W), outskirts (43.253235 N, 2.891099W) and city center (43.269326 N, 2.933702W).

Each sample was stored in dark glass bottles at −20 °C until analysis. The physicochemical parameters of the river water samples were reported in Table S1.

2.4. Photodegradation experiments

A cylindrical quart cell (i.d. 1.9 cm, length 10 cm, Hellma Italia, Milano, Italy) of 28.0 mL capacity was filled with the TNP ultrapure water solution (10.0 mg L^{-1}). The solar box was set at 600 W m^{-2} and a controlled temperature of 35 °C. The solution was exposed under stirring to a simulated sunlight irradiation on the water-cooled tray in the solarbox. The actual measured temperature of the sample was about 18–21 °C. These conditions were chosen considering the previous knowledge of the average irradiation and temperature in the period of July–September in the north of Spain, where the drug is available on prescription. A control sample was kept at room temperature and in dark conditions for the same time as the photodegradation experiments to further assess whether hydrolysis phenomena were present or not. Aliquots of the independent solutions (fifteen in total, 2 mL each) were withdrawn at different photodegradation times (0, 5, 10, 24, 29, 34, 48, 53, 58, 72, 77, 82, 96, 101 and 106 h, indicated from t_0 to t_{14}, respectively) and kept at −20 °C in amber glass vials until further UHPLC-MS/MS analysis. Before introducing and filling a fresh TNP solution into the quartz cell, the latter was emptied, and carefully and accurately cleaned.

2.5. Chromatographic and mass spectrometric conditions

The stationary phase used was an Acquity HSST3 C18 column (100 × 2.1 mm, 1.8 μm; Water Corporation, Milford, USA). The mobile phase was a mixture of water/acetonitrile 90/10 v/v (solvent A) and 10/90 v/v (solvent B) with the addition of 0.1 % (v/v) of formic acid. The mobile phase flow rate was 300 μL min^{-1} eluting in gradient mode as follows: 0.0–0.5 min, 5% solvent B; 0.5–6.0 min, 100% solvent B; 6.0–7.0 min, 100 % solvent B; 7.1 min, 5% solvent B; 7.1–10.0 min, 5% solvent B. The injection volume was 5 μL and the column oven temperature was set at 45 °C.

Accurate mass data were collected in positive ionization mode by data-independent acquisition MS^E, i.e., by alternating low and high energy applied to the collision cell. In the low-energy MS mode, data were collected at a constant collision energy of 6 V; in high-energy mode, the collision energy was ramped from 15 to 30 V with a scan time of 0.1 s. Spectra were recorded in the range of *m/z* 50–600. The source parameters were set as follows: electrospray capillary voltage 2.50 kV, sampling cone 10 V, and source and desolvation temperatures 140 °C and 600 °C, respectively. The cone and desolvation gas flows were 0 and 1000 L/h, respectively. Both in full and in MS/MS scan mode, a resolving power of 30,000 was used. The mass spectrometer was calibrated with sodium formate (0.5 M) and leucine-enkephalin (100 pg μL^{-1}) infused at 8 μL min^{-1} and acquired every 30 s as LockMass.

2.6. Preconcentration by solid phase extraction (SPE) procedure

Each river sample was centrifuged at 1500×*g* for 5 min to remove any suspended organic matter and the supernatant was filtered on 0.2 μm polytetrafluoroethylene (PTFE) filters (VWR, Radnor, USA). For the preconcentration of the four river samples, an SPE C18 cartridge from 1 mL to 100 mg (Phenomenex, Torrance, USA) was employed. First, the

cartridge was previously conditioned with 1.0 mL of methanol and 1.0 mL of ultrapure water. Then, 250 mL of each sample was loaded on the cartridge with an estimated flow of 1.3 mL min^{-1}. Then, the cartridge was dried for 5 min under vacuum and at least eluted with 2.0 mL of methanol. Each eluted solution was further evaporated to dryness with a gentle steam of nitrogen and reconstituted with 1.0 mL of mobile phase mixture at the initial gradient conditions previously described. With this SPE procedure, it is possible to reach a pre-concentration factor of 250x. The SPE preconcentration was replicated three times for each river sample.

3. Results and discussion

3.1. Development of the UHPLC-MS/MS method

A preliminary MS/MS characterization of TNP was conducted in order to obtain information from its MS/MS fragmentation potentially useful to further identify possible TPs formed during the irradiation experiments.

Both positive ionization (PI) and negative ionization (NI) modes were tested, but only in PI mode TNP was easily characterized thanks to the presence of nitrogen atoms in its structure. First, 0.2 mg L^{-1} solution of TNP in methanol was prepared from the stock solution and directly infused by a syringe pump at 0.1 μL min^{-1} into the mass spectrometer working in MS^E mode. The most intense signal for TNP in PI mode was *m/z* 437.1306 which corresponds to the [M+H]$^+$ species. The MS/MS spectrum and the related chemical structures for the more abundant product ions are reported in Fig. S2. It should be noted that the signal at *m/z* 292.0193 corresponds to the in-source fragmentation of the TNP molecule.

Thus, the QTOF MS/MS analyzer was used to develop a sensitive high-resolution MS/MS method for the study of the TNP photodegradation. For the quantification of the TNP high-resolution multiple reaction monitoring (HR-MRM) was used, considering the ion at *m/z* 437.1 as precursor ion and the ions at *m/z* 228.0381 and *m/z* 292.0204 as quantifier and qualifier product ions, respectively. Preliminary chromatographic analyses were carried out testing the separation performances of two different stationary phases, a Kinetex F5 (2.1 × 100 mm, 2.6 μm, Phenomenex, Torrance, USA) column and a Kinetex C18 XDB (100 × 3 mm, 1.7 μm, Phenomenex, Torrance, USA) column, that is able to elute the TNP and its TPs with gaussian peaks, avoiding tailing effect. However, TNP and one of TP (later named TP2) coeluted and therefore, the use of a functionalized C18 column such as Acquity HSST3 C18 column (100 × 2.1 mm, 1.8 μm; Water Corporation, Milford, USA) has proven successful, obtaining a good separation of these two peaks. Mixtures of methanol and acetonitrile with water were tested, in order to obtain an adequate separation of TNP and its TPs. ACN allows for shorter retention time, as well as resolved peaks, whereas the addition in the mobile phase of formic acid 0.1% improved the ionization of all the identified compounds. Fig. S3 shows, as an example, the extracted ion chromatogram (XIC) of TNP at *m/z* 437.1306 before (blue line) and after 106 h (magenta line) of irradiation. The peak of TNP at a retention time of 4.65 min decreased during degradation until it disappeared completely after prolonged irradiation in the solarbox and no other peaks, indicated afterward as TP1, TP2, etc., are visible to the naked eye. The other peaks present in the chromatogram correspond to the blank contribution.

Together with the most intense MS signal at 4.65 min (*m/z* 437.1306), there is another signal particularly intense at *m/z* 292.0193, that corresponds to the in-source fragmentation of TNP molecule, as reported also during the TNP MS/MS characterization.

3.2. Validation of the UHPLC-MS/MS method

For the validation of the method, standard solutions of TNP (0.100, 0.125, 0.250, 0.500, 1.0, 2.5, 5.0, 10, 25, 50, 100, 125 and 250 μg L^{-1})

were prepared to build a calibration model with weighting factor $1/x$, reporting the TNP chromatographic peak as dependent variable y and the standard concentrations as independent variable x. The quality of the model was evaluated by obtaining a determination coefficient (R^2) equal to 0.9927 in the range of 0.100–250 µg L^{-1}. The accuracy, expressed as the ratio of the calculated to the theoretical concentrations for the thirteen concentration levels was within the acceptable range of 90.5–108.5 %. The limit of detection (LOD) and the limit of quantification (LOQ) were calculated according to the International Council for Harmonization of Technical Requirements for Pharmaceuticals for Human Use guideline (ICH) as $3.3\sigma_{Blank}/b$ and $10\sigma_{Blank}/b$, respectively, being σ_{Blank} equals to the standard deviation of the blank, that is, the residual standard deviation ($\sigma_{y/x}$) and b the slope of the calibration model. The calculated LOD and LOQ were 0.030 µg L^{-1} and 0.100 µg L^{-1}, respectively (taking into account the preconcentration factor of the SPE procedure). Seven replicates of the blank river water sample were spiked with TNP solution at a concentration giving an S/N ratio between 2.5 and 5 to calculate the method detection limit (MDL) = $t_{(n-1, \alpha = 0.01)} \times s_d$, where $t = 3.14$ corresponds to a t-Student's value for 99% confidence level and six freedom degrees, and s_d is the standard deviation of the replicates. The method quantification limit (MQL) was defined as three times the MDL value. MDL and MQL were 0.030 and 0.100 µg L^{-1}, respectively, comparable to the values of LOD and LOQ obtained using TNP ultrapure water solutions.

Carry-over and memory effects were carefully evaluated, injecting a blank river sample after the injection of the TPN standard solution at 250 µg L^{-1} (the highest concentration level of the calibration plot). No carry-over or memory effects were found. In addition, selectivity was investigated by the analysis of 4 consecutive injections of the blank river water samples, replicated three times and no interfering species were observed at the retention time of the TNP and its TPs.

The repeatability was calculated by analyzing five times both the TNP ultrapure water solution at the concentration of the LOQ value and the blank river sample spiked with TNP solution at the concentration of MQL value, whereas the intermediate precision was determined by repeating the analyses for seven consecutive days of the week (a total of 35 analyses), respectively. The repeatability precision gave a relative standard deviation (RSD%) of the precision of the concentration lower than 4.8% and 5.2% calculated for TNP ultrapure water and spiked blank river sample, respectively, whereas the intermediate precision resulted always lower than 4.8%. As concerns the repeatability and the intermediate precision calculated for the retention time both for TNP in ultrapure water and spiked blank river samples, values always lower than 1.9% and 3.3% were obtained, respectively.

In order to evaluate the matrix effect (ME), calculated as $ME(\%) = \frac{slope_{add}}{slope_{ext}} \bullet 100 - 100$, a comparison between the slope of external calibration plot ($slope_{ext}$) and that of the standard addition plot ($slope_{add}$) was carried out through a t-test at a 95% confidence level. The standard addition plot was built by spiking a blank river water sample with the TNP standard solutions in the same concentration range as the external calibration model. No significant ME was found as reflected in the result of the t-test (equal to 0), i.e. the slopes of both models are not significant different at 95% from each other. The absence of matrix effect also confirms the absence of interfering compounds in the method and the achievement of the same identification and quantification limits both using solutions of TNP in ultrapure water (LOD and LOQ) and solutions of a blank river water sample (MDL and MQL). The recovery R was calculated as C_{exp}/C_{ref}, being C_{exp} the concentration of TNP determined after the UHPLC-MS/MS analysis and C_{ref} the concentration of a TNP spiked solution. TNP solutions were prepared at 0.6, 2.0 and 800 ng L^{-1} to explore the linearity range, considering the SPE pre-concentration factor of 250x. They were added to a blank river sample, which was submitted to the SPE procedure, replicating the analysis three times. The calculated R values for the three spiked concentration levels were (95.6

± 1.9)%, (106.8 ± 3.3)%, and (105.0 ± 5.3)%, and they were reproducible and independent of the TNP concentration in the explored concentration range, being not significantly different (as shown by a t-test at a 95% confidence level). Thus, the average recovery percentage ($R\%$) was (102.5 ± 3.5)%. By following this SPE procedure, it is possible to quantify the TNP in water down to a concentration of 400 pg L^{-1}.

3.3. Photodegradation experiments

To assess the degradation of TNP in ultrapure water, each solution withdrawn at different times, (according to the information reported in section 2.4) was analyzed with the developed UHPLC-MS/MS method. Then, the chromatographic peak area of TNP was calculated from the XIC at each degradation time for the m/z 437.1306. The results of the irradiation of TNP standard solution up to 106 h showed that TNP photodegradation kinetics was of the pseudo-first-order (Fig. S4). Towards 72 h of irradiation (t_9), the chromatographic peak of TNP at 4.65 min drastically decreased and after 106 h of irradiation (t_{14}), it decreased up to 99% of the initial intensity (t_0), that is, before exposition in the solarbox. The first-order constant (k) of TNP in ultrapure water is 0.0575 ± 0.0096 h^{-1} and the half-life time ($t_{1/2}$) is 12.0 ± 2.4 h. Afterward, the same degradation experiments were carried out spiking a blank river water sample with a TNP solution at 0.8 µg L^{-1}. The withdrawn aliquot after irradiation was subjected to SPE pre-concentration procedure and submitted to UHPLC-MS/MS analysis. The resulting kinetics is very similar to that obtained in ultrapure water, taking into account the possible influence of the matrix on the degradation (k = 0.065 ± 0.014, $t_{1/2}$ = 10.6 ± 2.6 h).

In addition, no evidence of hydrolysis reactions was found for the control sample kept in the dark at room temperature during the irradiation experiments, since neither the formation of hydrolytic products nor the decrease of the TNP peak area was observed. The chromatographic profile of the control solution is identical to that depicted in Fig. S3 for the TNP standard solution no subjected to irradiation (t_0), which was frozen until further analysis.

3.4. Identification of TPs

For the identification of potential TPs, a project was made in MS-Dial software including all the MS/MS data from t_1 to t_{14}, using t_0 as a reference for peak alignment. The tolerance parameters imposed for the alignment were 0.1 min for the retention time and 0.015 Da for the m/z. The ratio of the sample peak area to that of the reference (t_0) must be greater than 10 times to be considered a TP of the TNP. A chromatographic peak list was then created including all the possible m/z candidates. By following this procedure, among all the large MS/MS datasets, eight TPs were found. Fig. 1 shows the XIC for each identified TP in ultrapure water. Signals have been min-max scaled for visual purposes, so they can be easily compared. As can be seen, all peaks are well resolved with respect to the TNP chromatographic peak, except for TP4 at 4.61 min. Nevertheless, as the acquisition mode of the MS and MS/MS spectra was data-independent, a proper characterization of the related precursor ion for TP4 was efficiently made. TP5, TP6 and TP7 have almost similar m/z values but at different retention times.

Following the same procedure described in subsection 3.3, the trends of signal area versus degradation time were plotted, as shown in Fig. 2. As can be seen, they all follow a logical increase-decrease pattern through time, with a sharp increase in the first 10 h, followed by an approximately sharp decline until close to disappearance within 106 h, except for TP1 and TP3, whose area values and therefore the concentrations in solution are still high after 106 h. This behavior could be attributed to the fact that they are sub-products of other TPs.

For the characterization of the chemical structures of the unknown TPs, by using MS-finder software, we based on the molecular formula
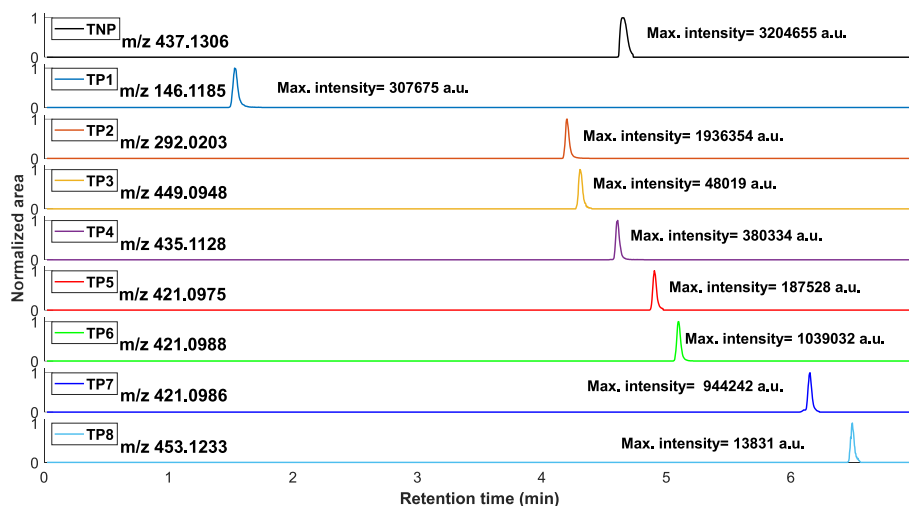
Fig. 1. Extracted ion chromatogram for TNP (black trace) and TPs (color traces). Intensities are min-max scaled. (For interpretation of the references to color in this figure legend, the reader is referred to the Web version of this article.)
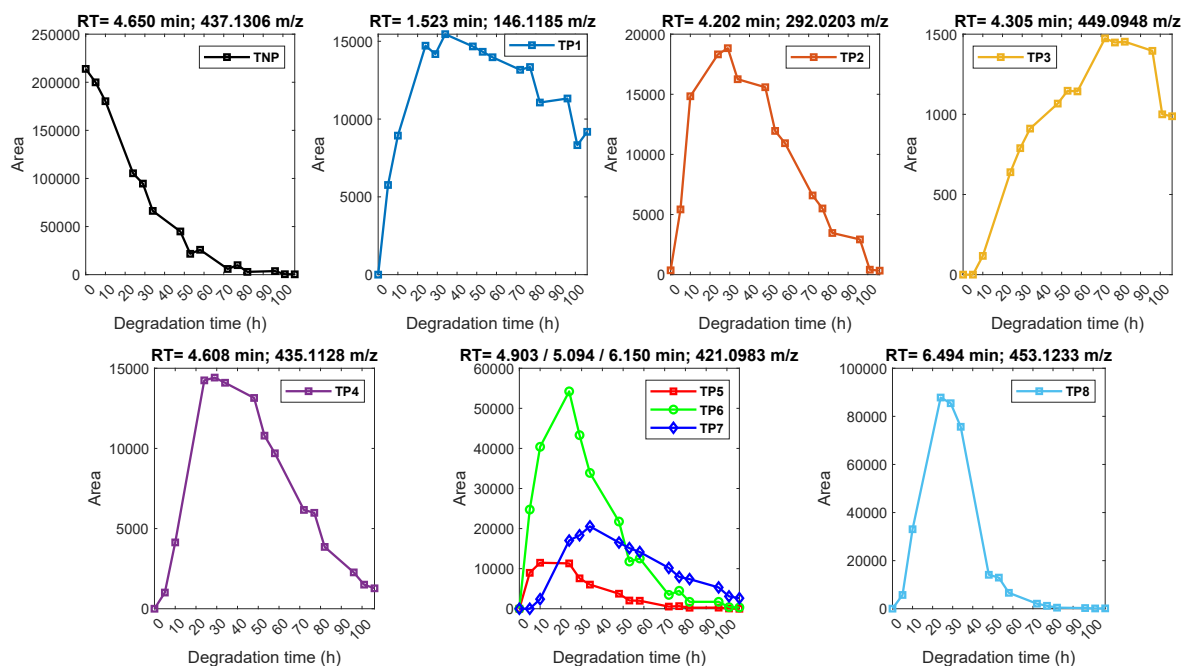

Fig. 2. Evolution profile of TNP and the eight most abundant TPs.

within the average MS accuracy of around 2 ppm, the relative abundance of the isotopic cluster within a tolerance of 10%, the number of rings and double bonds (RDBs) and the use of the high-accurate and high-resolution MS/MS acquired spectra, which average mass tolerance for each product ion was within 10.4 ppm. Thus, the interpretation of the precursor molecular structure has been particularly made based on the MS/MS fragmentation. All the related information is summarized in Table 1.

All the characterized TPs have not been previously identified in the literature, thus all the chemical structures of TPs have been completely hypothesized based on the HR-MS/MS of the current study. All MS/MS spectra from TP1 to TP8 are reported in the Supplementary Material with the identification of the most abundant m/z signals.

First of all, it can be seen that the TNP molecule breaks into two parts by splitting the aliphatic chain part (giving rise to TP1) and the tricyclic structure part to form TP2. Therefore, TP1 could be attributed to the amino-carboxylic acid chain of TNP, after the cleavage between the

amino group and the carbon in α of the cycloheptane ring (Fig. S5). As seen in Fig. 3 and considering the information extracted from the evolution plots in Fig. 2, we proposed this TP as a likely byproduct of other TPs, in particular TP4, TP6, TP7 and TP8.

On the contrary, TP2 formed by the loss of the TP1 from TNP: it is both an in-source fragmentation, as previously seen with the same chromatographic peak as TNP (RT = 4.65 min), and a TP whose chromatographic peak is not present in either the control or t_0 sample (RT = 4.20 min). The MS/MS spectrum for the precursor ion at m/z 292.0203 (RT = 4.20 min) is shown in Fig. S6.

TP3 is the product of ketone formation on the α-carbon with respect to the aliphatic amine, which also forms a double bond with the ring. It is also possible to form the ketone in the β- or even γ-carbon. However, we considered these possibilities as less likely to occur, since the chemical structure proposed for the product ion of TP3 at m/z 240.1233 (Fig. S7) consists of the cleavage of the N–S bond, followed by the loss of SO_2 and Cl with radical formation, reinforcing the fact of ketone
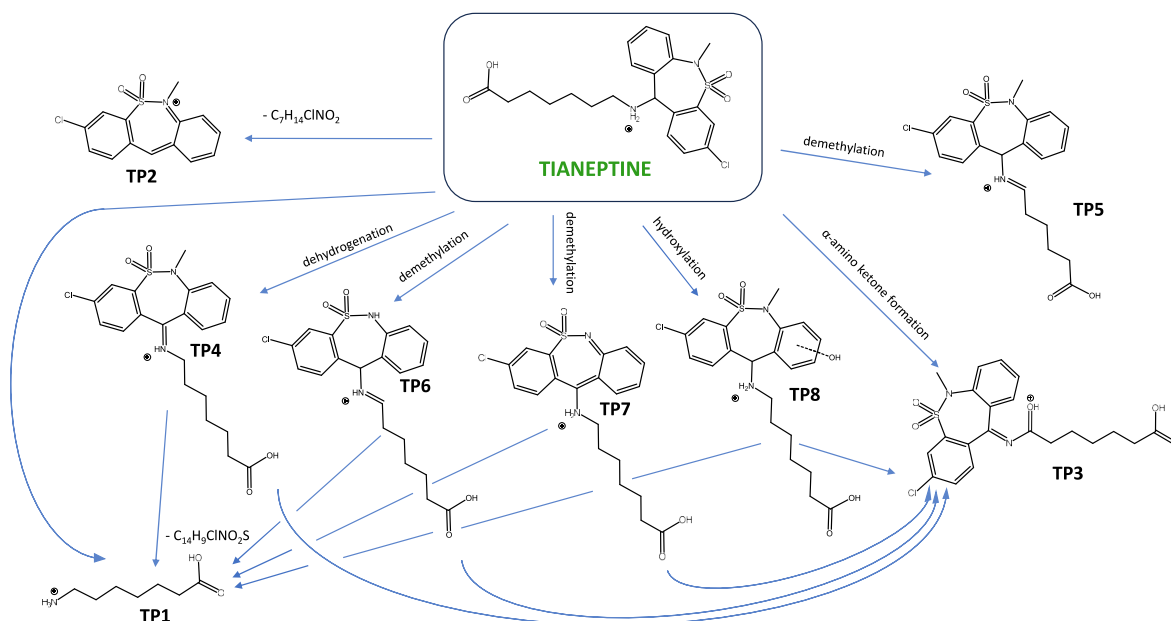
Fig. 3. Proposed mechanism of reactions involved in the photodegradation of TNP.

formation in the α-carbon. Considering this product ion, the only possibility for β-formation is also the methyl group loss of the amine in the ring, which is more unlikely. Similar considerations can be made for the product ion at *m/z* 133.0146 (Fig. S7). As for TP1, we propose this TP as a byproduct of TP4, TP6, TP7 and TP8.

We proposed TP4 as an imine, which can be further degraded to form TP1. This hypothesis can be confirmed by the proposed structures of the TP4 product ion signals at *m/z* 339.1407, *m/z* 308.0331 and in particular at *m/z* 307.0293 (Fig. S8).

TP5, TP6 and TP7 have almost the same *m/z* (421.075, 421.0988, 421.0986, respectively), with a maximum mass error of 3.1 ppm between TP5 and TP6. They are three structural isomers, whose MS/MS spectra are very similar to each other (Fig. S9, S10 and S11) and their retention times (as can be seen in Fig. 1) are relatively close.

Their chemical structures were proposed on the basis of the interpretation of MS/MS spectra. In particular, the signals at *m/z* 206.1906 (Fig. S10) and *m/z* 275.9886 (Fig. S11), related to the product ions of TP6 and TP7 respectively, can only be assigned to the brute formula $C_{14}H_{24}N$ with an acceptable accuracy value (−1.33 ppm) and $C_{13}H_7ClNO_2S$ (1.98 ppm), respectively. The chemical structure proposed for the *m/z* 206.1906 includes the amino aliphatic chain with the loss of the carboxylic group: being six the total number of carbons in the chain, it is not possible for TP5, whose aliphatic chain was proposed with 5 carbon atoms. Additional TPs with even a smaller number of carbons in the chains have not been identified in the photodegradation of TNP, such as that with 5 carbon atoms in the chain, reported in the literature as one of the main metabolites of TNP found in urine (Horlachuk et al., 2019).

Moreover, the proposed structures for TP6 and TP7 are the only ones which have lost the methyl linked to the nitrogen atom of the dibenzothiazepine core. In TP6, is the aliphatic amine the one with a double bond, whereas in TP7, is the cyclic amine the one with a double bond.

Finally, TP8 is the hydroxylation of the benzene close to the cyclic amine. Unfortunately, as can be seen in Fig. S12, there is not enough information to confirm the hydroxylation position.

The UHPLC-MS/MS analyses carried out on the irradiated blank river water sample, previously spiked with TNP at 10.0 mg L^{-1}, showed the presence of the same TPs as those formed during the irradiation of TNP ultrapure water solution.

3.5. River water samples analysis

The developed and validated method was successfully applied to the analysis of the four river water samples from Nervión River (Bilbao, Spain), after the pre-concentration step to identify and quantify the possible presence of TNP and any TPs. Despite the increasing use and abuse of TNP (El Zahran et al., 2018), the consoling fact is that neither TNP nor any TPs were found in the four analyzed samples. The explanation could be that, contrary to what is reported in the literature and limited to the analyzed water samples from the Nervión River, the use and abuse of TNP in this area is not very frequent. Furthermore, it must be considered that TNP is metabolized in the human body, being the unchanged molecule contribution in urine less than 3%, after 24 h of a single dose administration (Horlachuk et al., 2019). However, a more extensive sampling campaign of rivers from different Countries where the use of this drug is still present should be done in order to make assumptions on the real consumption or the presence of unchanged TNP or any TPs in rivers. Nevertheless, the retrospective analysis of UHPLC-MS/MS data highlighted the presence of 1409 unknown peaks (signal-to-noise ratio higher than 100) among which it was been possible to identify three molecules of interest present in the analyzed river water samples which match the library NIST used (Table S2).

The first identified molecule with a satisfactory similarity percentage with respect to the NIST spectral library was 11-hydroxy-Δ9-THC, the main metabolite of Δ9-tetrahydrocannabinol (Δ9-THC), which was found in all four samples, but mainly in the sample collected in the city center (sample 4), where consumption of cannabinoids is expected to be high.

The second identified molecule was 4-methyl-7-(diethylamino) coumarin and it was mainly found in the river mouth and the outskirts samples (samples 1 and 3, respectively). Coumarin and its derivates constitute a major class of fluorescent organic dyes.

The third identified molecule was tetrabutylammonium, which was mainly found in the river mouth and the industrial area samples (samples 1 and 2, respectively). Tetrabutylammonium is usually presented in the form of diverse salts, and its use is very widespread as a synthesis reagent, therefore often associated with the disposal of wastewater from industrial areas.

3.6. Toxicity assessment of TNP and TPs

Environmental influence and the toxicity of TNP and its TPs were evaluated *in silico*, by means of quantitative structure-activity relationships (QSARs) and read-across models implemented in the free available internet resources Toxicity Estimation Software Tool (T.E.S.T) (Toxicity Estimation Software Tool) and VEGA (VEGA QSAR) software.

On the one hand, using the Simplified Molecular Input Line Entry System (SMILES) notation as input, T.E.S.T. software was used to predict the acute aquatic toxicity on fish (LC50-96 h), *Daphnia magna* (LC50-48 h), *Tetrahymena pyriformis* (IGC50-48 h) and the acute oral toxicity on rat (LD50) following the consensus method and relaxing the fragment constraint in all cases. On the other hand, mutagenicity (consensus method), developmental toxicity, bioaccumulation, ready biodegradability and persistence in water, soil and sediments were predicted by VEGA software, also using the SMILES notation. Predicted values are reported in Table S3.

An exploratory analysis of the data was performed by means of principal component analysis (PCA), whose scores and loadings plots for the first two principal components (PCs) are shown in (Fig. S13). The projection of the *in silico* predictions in the orthogonal space leads to 76% of the total data variance explained in the first two PCs.

PC1 explains the difference between TP1 (negative scores), characterized by low toxicity values and readily biodegradable, and the rest of the TPs and TNP (positive scores), for which persistence in the sediments and bioaccumulation are the most characteristic variables. PC2 mainly highlights the differences in terms of persistence in water and soil (negative loadings) versus the persistence in sediments (positive loadings). Indeed, TP2 which has negative scores in PC2 has the highest soil persistence predicted value, whereas TP6 (positive score values in PC2) shows the lowest persistence in water. At least, most TPs exhibit the same mutagenicity (except for TP4) and developmental toxicity as TNP, which are the two variables with loadings close to zero in both PCs.

According to the Globally Harmonized System (GHS) of classification and labelling of chemicals (United Nations), TNP and its TPs, are predicted as moderately toxic for aquatic environments and classified into the Category Acute 1 ($96\,h\,LC_{50} \leq 1\,mg\,L^{-1}$) except for TP1, classified as Category Acute 3 ($10\,mg\,L^{-1} < 96\,h\,LC_{50} \leq 100\,mg\,L^{-1}$). Considering the toxicity in rats by oral ingestion, most of the samples are labelled as Category 4 ($300\,mg\,kg^{-1} < LD_{50} \leq 2000\,mg\,kg^{-1}$) except for TP2, classified as Category 5 ($2000\,mg\,kg^{-1} < LD_{50} \leq 5000\,mg\,kg^{-1}$). In addition, most of TPs were predicted as interfering potential for the normal development of humans or animals, especially true for TP1 prediction with good reliability. According to REACH regulation EC No 1907/2006, most of them have a low potential of bioaccumulation (log BFC <3.3), with the only exception being TP4, therefore labelled as poorly persistent in aquatic and terrestrial environments.

4. Conclusion

The irradiation experiments by direct photolysis through simulated sunlight carried out in this study proved to be a powerful methodology for the assessment of TNP TPs in ultrapure and surface water. The degradation kinetics of TNP in both matrices are very similar, as well as the identified TPs, although other influencing parameters on the kinetic of photodegradation such as pH, total dissolved organic matter or major inorganic ions will have to be taken into account in further irradiation experiment studies. Nevertheless, the methodology presented was solid enough to elucidate eight TPs not previously found in the literature, following the high-resolution MS/MS data analysis approach. The proposed degradation mechanism for TNP, which is based on the elucidation of the TPs discussed in the text, evidences that two of the TPs (TP1 and TP3) are degraded both from TNP and the other TPs, which can be an important clue for future studies of TNP occurrence in natural waters. In general, TPs were of comparable toxicity to TNP, with a few exceptions due to TP1 (less toxic), TP2 much more persistent in soil, TP6 not

very persistent in water, and TP4 which was positive in the Ames mutagenicity test. Among the four water samples analyzed in this study (Nervión River), no TNP or any of the TPs were found. However, additional analyses should be conducted in the future by increasing the number of samples and sampling points to obtain a better perspective of the fate of TNP in natural waters where consumption is still present and legal nowadays.

CRediT authorship contribution statement

Enmanuel Cruz Muñoz: Writing – original draft, Visualization, Investigation, Formal analysis, Data curation. **Veronica Termopoli:** Writing – review & editing. **Marco Orlandi:** Writing – review & editing, Funding acquisition. **Fabio Gosetti:** Writing – review & editing, Visualization, Validation, Supervision, Project administration, Methodology, Investigation, Conceptualization.

Declaration of generative AI and AI-assisted technologies in the writing process

During the preparation of this work, the author(s) did not use any service based on AI-assisted technologies.

Declaration of competing interest

The authors declare the following financial interests/personal relationships which may be considered as potential competing interests: Fabio Gosetti reports financial support was provided by European Union. Veronica Termopoli reports financial support was provided by European Union. Marco Orlandi reports financial support was provided by European Union. If there are other authors, they declare that they have no known competing financial interests or personal relationships that could have appeared to influence the work reported in this paper.

Data availability

Data will be made available on request.

Appendix A. Supplementary data

Supplementary data to this article can be found online at https://doi.org/10.1016/j.chemosphere.2024.142534.

References

Bavumiragira, J.P., Ge, J., Yin, H., 2022. Fate and transport of pharmaceuticals in water systems: a processes review. Sci. Total Environ. 823, 153635 https://doi.org/10.1016/j.scitotenv.2022.153635.

Boogaerts, T., Degreef, M., Covaci, A., van Nuijs, A.L.N., 2019. Development and validation of an analytical procedure to detect spatio-temporal differences in antidepressant use through a wastewater-based approach. Talanta 200, 340–349.

Bottaro, M., Frascarolo, P., Gosetti, F., Mazzucco, E., Gianotti, V., Polati, S., Pollici, E., Piacentini, L., Pavese, G., Gennaro, M.C., 2008. Hydrolytic and photoinduced degradation of Tribenuron methyl studied by HPLC-DAD-MS/MS. J. Am. Soc. Mass Spectrom. 19, 1221–1229. https://doi.org/10.1016/j.jasms.2008.05.009.

Brieudes, V., Lardy-Fontan, S., Vaslin-Reimann, S., Budzinski, H., Lalere, B., 2017. Development of a multi-residue method for scrutinizing psychotropic compounds in natural waters. J. Chromatogr. B. 1047, 160–172. https://doi.org/10.1016/j.jchromb.2016.07.016.

Calisto, V., Esteves, V.I., 2009. Psychiatric pharmaceuticals in the environment. Chemosphere 77, 1257–1274. https://doi.org/10.1016/j.chemosphere.2009.09.021.

Calza, P., Jiménez-Holgado, C., Coha, M., Chrimatopoulos, C., Dal Bello, F., Medana, C., Sakkas, V., 2021. Study of the photoinduced transformations of sertraline in aqueous media. Sci. Total Environ. 756, 143805 https://doi.org/10.1016/j.scitotenv.2020.143805.

Chen, H.-W., Liu, H.-T., Kuo, Y.-N., Yang, D.-P., Ting, T.-T., Chen, J.-H., Chiu, J.-Y., Jair, Y.-C., Li, H.-C., Chiang, P.-J., Chen, W.-R., Lin, M.-C., Hsu, Y.-H., Chen, P.-S., 2023. Rapid and sensitive dilute-and-shoot analysis using LC-MS-MS for identification of multi-class psychoactive substances in human urine. J. Pharm. Biomed. Anal. 233, 115443 https://doi.org/10.1016/j.jpba.2023.115443.

Diaz-Camal, N., Cardoso-Vera, J.D., Islas-Flores, H., Gómez-Oliván, L.M., Mejía-García, A., 2022. Consumption and occurrence of antidepressants (SSRIs) in pre- and post-COVID-19 pandemic, their environmental impact and innovative removal methods: a review. Sci. Total Environ. 829 https://doi.org/10.1016/j.scitotenv.2022.154656.

Duan, S., Fu, Y., Dong, S., Ma, Y., Meng, H., Guo, R., Chen, J., Liu, Y., Li, Y., 2022. Psychoactive drugs citalopram and mirtazapine caused oxidative stress and damage of feeding behavior in Daphnia magna. Ecotoxicol. Environ. Saf. 230, 113147 https://doi.org/10.1016/j.ecoenv.2021.113147.

El Zahran, T., Schier, J., Glidden, E., Kieszak, S., Law, R., Bottei, E., Aaron, C., King, A., Chang, A., 2018. Characteristics of tianeptine exposures reported to the national poison data system — United States, 2000–2017. MMWR Morb. Mortal. Wkly. Rep. 67, 815–818. https://doi.org/10.15585/mmwr.mm6730a2.

Fong, P.P., Molnar, N., 2013. Antidepressants cause foot detachment from substrate in five species of marine snail. Mar. Environ. Res. 84, 24–30. https://doi.org/10.1016/j.marenvres.2012.11.004.

García-García, P., 2016. Tianeptine, antidepressant with positive benefit/risk. Rev. Psiquiatía Salud Ment. 9, 234–235. https://doi.org/10.1016/j.rpsmen.2016.07.002.

Giebułtowicz, J., Nałecz-Jawecki, G., 2014. Occurrence of antidepressant residues in the sewage-impacted Vistula and Utrata rivers and in tap water in Warsaw (Poland). Ecotoxicol. Environ. Saf. 104, 103–109. https://doi.org/10.1016/j.ecoenv.2014.02.020.

Gornik, T., Carena, L., Kosjek, T., Vione, D., 2021a. Phototransformation study of the antidepressant paroxetine in surface waters. Sci. Total Environ. 774, 145380 https://doi.org/10.1016/j.scitotenv.2021.145380.

Gornik, T., Shinde, S., Lamovsek, L., Koblar, M., Heath, E., Sellergren, B., Kosjek, T., 2021b. Molecularly imprinted polymers for the removal of antidepressants from contaminated wastewater. Polymers 13, 1–20. https://doi.org/10.3390/polym13010120.

Gosetti, F., Chiuminatto, U., Zampieri, D., Mazzucco, E., Marengo, E., Gennaro, M.C., 2010. A new on-line solid phase extraction high performance liquid chromatography tandem mass spectrometry method to study the sun light photodegradation of mono-chloroanilines in river water. J. Chromatogr., A 1217, 3427–3434. https://doi.org/10.1016/j.chroma.2010.02.080.

Gosetti, F., Chiuminatto, U., Mazzucco, E., Mastroianni, R., Bolfi, B., Marengo, E., 2015. Ultra-high performance liquid chromatography tandem high-resolution mass spectrometry study of tricyclazole photodegradation products in water. Environ. Sci. Pollut. Res. 22, 8288–8295. https://doi.org/10.1007/s11356-014-3983-4.

Gosetti, F., Bolfi, B., Chiuminatto, U., Manfredi, M., Robotti, E., Marengo, E., 2018. Photodegradation of the pure and formulated alpha-cypermethrin insecticide gives different products. Environ. Chem. Lett. 16, 581–590. https://doi.org/10.1007/s10311-017-0685-4.

Gosetti, F., Belay, M.H., Marengo, E., Robotti, E., 2020. Development and validation of a UHPLC-MS/MS method for the identification of irinotecan photodegradation products in water samples. Environ. Pollut. 256, 113370 https://doi.org/10.1016/j.envpol.2019.113370.

Gros, M., Williams, M., Llorca, M., Rodriguez-Mozaz, S., Barceló, D., Kookana, R.S., 2015. Photolysis of the antidepressants amisulpride and desipramine in wastewaters: identification of transformation products formed and their fate. Sci. Total Environ. 530–531, 434–444. https://doi.org/10.1016/j.scitotenv.2015.05.135.

N. Horlachuk, I. Halkevych, L. Logoyda, L. Mosula, N. Zarivna, O. Polyauk, Chromatography-mass spectrometry analysis of tianeptine in urine, Int. J. Green Pharm. 13 (2019) 87. http://prime.psc.riken.jp/, (n.d.).

Hu, Z., Li, J., Xiao, A., Zheng, J., Guan, S., Guo, J., Huang, M., 2022. Development and validation of UHPLC-MS/MS method for simultaneous quantification of escitalopram and its major metabolites in human plasma and its application in depressed patients. J. Pharm. Biomed. Anal. 217, 114810 https://doi.org/10.1016/j.jpba.2022.114810.

ICH, ICH HARMONISED TRIPARTITE GUIDELINE VALIDATION OF ANALYTICAL PROCEDURES: Q2(R1), in: n.d. https://database.ich.org/sites/default/files/Q2%28R1%29Guideline.pdf.

ISO, 2014. Guideline ISO 5667-6:2014; Water quality—sampling—Part 6: guidance on sampling of rivers and streams. https://www.iso.org/standard/55451.html.

Italian Ministry of Health, 2020. GU Serie Generale n. 85 del 30-03-2020. https://www.gazzettaufficiale.it/eli/gu/2020/03/30/85/sg/pdf.

Khedr, A., 2007. High-performance liquid chromatographic stability indicating assay method of tianeptine sodium with simultaneous fluorescence and UV detection. J. Chromatogr. Sci. 45, 305–310. https://doi.org/10.1093/chromsci/45.6.305.

Ma, Y., Xu, D., Li, C., Wei, S., Guo, R., Li, Y., Chen, J., Liu, Y., 2022. Combined toxicity and toxicity persistence of antidepressants citalopram and mirtazapine to zooplankton Daphnia magna. Environ. Sci. Pollut. Res. 29, 66100–66108. https://doi.org/10.1007/s11356-022-20203-3.

Metcalfe, C.D., Chu, S., Judt, C., Li, H., Oakes, K.D., Servos, M.R., Andrews, D.M., 2010. Antidepressants and their metabolites in municipal wastewater, and downstream exposure in an urban watershed. Environ. Toxicol. Chem. 29, 79–89. https://doi.org/10.1002/etc.27.

Osawa, R.A., Carvalho, A.P., Monteiro, O.C., Oliveira, M.C., Florêncio, M.H., 2019. Transformation products of citalopram: identification, wastewater analysis and in silico toxicological assessment. Chemosphere 217, 858–868. https://doi.org/10.1016/j.chemosphere.2018.11.027.

Pivetta, R.C., Rodrigues-Silva, C., Ribeiro, A.R., Rath, S., 2020. Tracking the occurrence of psychotropic pharmaceuticals in Brazilian wastewater treatment plants and surface water, with assessment of environmental risks. Sci. Total Environ. 727, 138661 https://doi.org/10.1016/j.scitotenv.2020.138661.

Rejek, M., Grzechulska-Damszel, J., 2018. Degradation of sertraline in water by suspended and supported TiO2. Polish J. Chem. Technol. 20, 107–112. https://doi.org/10.2478/pjct-2018-0030.

Sindu, P., 2020. Management of depression with behavior therapy. Curr. Res. Behav. Sci. 1, 100001 https://doi.org/10.1016/j.crbeha.2020.100001.

Subedi, B., Kannan, K., 2015. Occurrence and fate of select psychoactive pharmaceuticals and antihypertensives in two wastewater treatment plants in New York State, USA. Sci. Total Environ. 514, 273–280. https://doi.org/10.1016/j.scitotenv.2015.01.098.

Świacka, K., Maculewicz, J., Kowalska, D., Caban, M., Smolarz, K., Śwież ak, J., 2022. Presence of pharmaceuticals and their metabolites in wild-living aquatic organisms – current state of knowledge. J. Hazard Mater. 424, 127350 https://doi.org/10.1016/j.jhazmat.2021.127350.

Toxicity Estimation Software Tool (T.E.S.T.), Ver. 5.1.2, Available online: https://www.epa.gov/chemical-research/toxicity-estimation-software-tool-test.

Trawiński, J., Skibiński, R., 2017. Studies on photodegradation process of psychotropic drugs: a review. Environ. Sci. Pollut. Res. 24, 1152–1199. https://doi.org/10.1007/s11356-016-7727-5.

United Nations, Globally Harmonized System of Classification and Labelling of Chemicals (GHS)., Available online: https://unece.org/sites/default/files/2021-09/GHS_Rev9E_0.pdf.

UNODC, 2023. Addicts and Consumers of Illegal Drugs Worldwide from 1990 to 2020 (In Millions). Statista [Graph]. https://www.statista.com/statistics/274688/addicts-and-consumers-of-illegal-drugs-worldwide/.

Valdez, C.A., Rosales, J.A., Leif, R.N., 2023. Determination of fentanyl and acetylfentanyl in soil in their intact form and orthogonal corroboration of their presence by EI-GC-MS using chloroformate chemistry. Forensic Chem 34, 100504. https://doi.org/10.1016/j.forc.2023.100504.

VEGA QSAR, ver. 1.2.0. Available online: https://www.vegahub.eu/portfolio-item/vega-qsar/.

Verlicchi, P., Al Aukidy, M., Zambello, E., 2012. Occurrence of pharmaceutical compounds in urban wastewater: removal, mass load and environmental risk after a secondary treatment-A review. Sci. Total Environ. 429, 123–155. https://doi.org/10.1016/j.scitotenv.2012.04.028.

W AJ, O D, S CM, 2001. Tianeptine: a review of its use in depressive disorders. CNS Drugs 15, 231–259. http://limo.libis.be/resolver?&sid=EMBASE&issn=11727047&id=doi:&atitle=Tianeptine%3A+A+review+of+its+use+in+depressive+disorders&stitle=CNS+Drugs&title=CNS+Drugs&volume=1.

Xu, D., Ji, J., Xiang, P., Yan, H., Zhang, W., Shen, M., 2023. Determination of 5 synthetic cannabinoids in hair by Segmental analysis using UHPLC-MS/MS and its application to eight polydrug abuse cases. Forensic Sci. Int. 346, 111611 https://doi.org/10.1016/j.forsciint.2023.111611.

Yang, H., Lu, G., Yan, Z., Liu, J., Dong, H., 2018. Influence of suspended sediment characteristics on the bioaccumulation and biological effects of citalopram in Daphnia magna. Chemosphere 207, 293–302. https://doi.org/10.1016/j.chemosphere.2018.05.091.

Zaki, M.F., Wu, Y.-H., Chen, P.-C., Chen, P.-S., 2023. Determination of psychoactive substances in one microliter plasma using a novel 3D printing microfluidic paper-based column coupled to liquid chromatography-mass spectrometry. Sensors Actuators B Chem 393, 134243. https://doi.org/10.1016/j.snb.2023.134243.